Computers and Structures 131 (2014) 81–97

Contents lists available at ScienceDirect

Computers and Structures

journal homepage: www.elsevier.com/locate/compstruc

Towards a procedure to automatically improve finite element solutions by interpolation covers

Jaehyung Kim, Klaus-Jürgen Bathe *

Department of Mechanical Engineering, Massachusetts Institute of Technology, Cambridge, MA 02139, USA

ARTICLE INFO

Article history:
Received 12 August 2013
Accepted 26 September 2013
Available online 7 November 2013

Keywords:
Finite elements
3-Node triangular element
4-Node tetrahedral element
Improvement of displacements and stresses
Interpolation covers
Enrichment of interpolations

ABSTRACT

In a previous paper (Kim and Bathe, 2013) [1], we introduced a scheme to improve finite element displacement and stress solutions by the use of interpolation covers. In the present paper we show how the scheme can be used to *automatically* improve finite element solutions. As in Ref. (Kim and Bathe, 2013) [1], we focus on the use of the low-order finite elements for the analysis of solids, namely, the 3-node triangular and 4-node tetrahedral elements with the use of interpolation covers. An error indicator is employed to automatically establish which order cover to apply at the finite element mesh nodes to best improve the accuracy of the solution. Some two- and three-dimensional problems are solved to illustrate the procedure.

1. Introduction

In standard finite element analysis, the numerical solution is improved by changing the locations of the mesh nodes, increasing the mesh density, or as another option, using a more powerful element. A scheme to proceed differently has been discussed in Ref. [1]. This method uses interpolation covers over patches of elements to enrich the displacement interpolations and increase the solution accuracy. The order of the interpolations can vary depending on what improvement in accuracy is needed. The scheme is closely related to the numerical manifold method proposed by Shi [2,3]. We refer to Ref. [1] for a detailed description of the scheme using interpolation covers and further references pertaining to its development.

The scheme was established in detail to improve the stress solutions when using the 3-node triangular element in two-dimensional analyses and the 4-node tetrahedral element in three-dimensional analyses. The use of these classical elements is attractive because these elements can be used to mesh very complex geometries, and they are robust and lead to relatively small bandwidths, but almost always it would be of much value to have better stress predictions [4,5].

The objective in the present paper is to use the scheme of Ref. [1] and present a fully automatic procedure to adaptively choose the orders of the interpolation covers with the aim to increase the solution accuracy for meshes using the low-order elements. Since the interpolation covers are compatible in displacements, an arbitrary combination of covers and order of interpolations can be chosen. Of course, an *ideal* adaptive scheme should give more accuracy at a smaller computational cost than using the traditional approach of using a finer mesh or higher-order finite elements.

In the adaptive interpolation procedure, we shall use cover orders up to cubic, to provide a flexible adaptive range. We focus our discussion on the analysis of problems in solid mechanics, but similar ideas can directly be applied to the analysis of problems in heat transfer, fluid flow and multiphysics.

In the following sections, we first briefly review the scheme using interpolation covers to improve the accuracy of solutions, we then present the adaptive scheme to automatically choose the covers, and finally we give example solutions to illustrate the performance of the method.

2. The finite element formulation enriched with covers

In this section, we briefly review the finite element formulation enriched with covers for low-order elements, merely to provide the foundation for the sections to follow. A detailed description also referring to other related research works is given in Ref. [1].

Let us assume that a mesh of 3-node triangular (or 4-node tetrahedral) elements has been used to obtain a displacement and stress solution of a two-dimensional (or three-dimensional) problem in solid mechanics. Fig. 1(a) shows a node i, the two-dimensional elements connected to that node and the linear interpolation function h_i used in the solution. We define C_i to be

* Corresponding author. Tel.: +1 6179265199.
E-mail address: kjb@mit.edu (K.J. Bathe).

0045-7949/$ - see front matter © 2013 Elsevier Ltd. All rights reserved.
http://dx.doi.org/10.1016/j.compstruc.2013.09.007

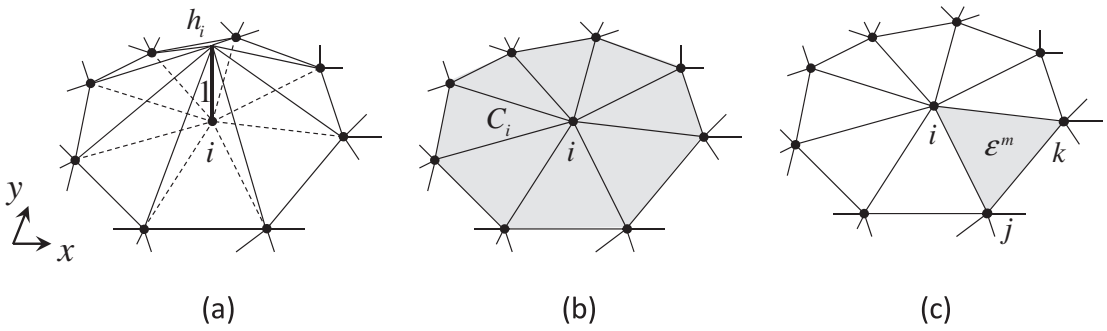

Fig. 1. Schematic description of sub-domains for enriched interpolations: (a) usual linear nodal shape function, (b) cover region or elements affected by the interpolation cover, and (c) an element.

the support domain of h_i and call C_i the *cover region*, as seen in Fig. 1(b).

To enrich the standard finite element interpolation for the solution of a variable u, we use interpolation cover functions, that is, over each cover region C_i, we assign an additional and enriching interpolation. Let u_i be the usual nodal variable for the solution of u, then we use, correspondingly, the polynomial bases of degree p over the cover region C_i given by

$$\mathcal{P}_i^p[u] = u_i + \begin{bmatrix} \bar{x}_i & \bar{y}_i & \bar{x}_i^2 & \bar{x}_i\bar{y}_i & \bar{y}_i^2 & \cdots & \bar{y}_i^p \end{bmatrix} \mathbf{a}_i \tag{1}$$

In Eq. (1), the coordinate variables $(\bar{x}_i, \bar{y}_i)$ are measured from node i and the vector $\mathbf{a}_i = [\, a_{i1} \quad a_{i2} \quad \cdots]^T$ lists additional degrees of freedom at node i for the cover region C_i. A normalization of the degrees of freedom can here be introduced by using $a_{ij}/(\widehat{h})^q$ for the terms of order q, where $\widehat{h}$ is a characteristic element length scale of the elements used.

With the above definitions, the enriched cover approximation of a field variable u for an element is

$$u = \sum_{i=1}^{3} (h_i u_i + \mathbf{H}_i \mathbf{a}_i) \tag{2}$$

where

$$\mathbf{H}_i = h_i \begin{bmatrix} \bar{x}_i & \bar{y}_i & \bar{x}_i^2 & \bar{x}_i\bar{y}_i & \bar{y}_i^2 & \cdots & \bar{y}_i^p \end{bmatrix} \tag{3}$$

and the sum is taken over the three local finite element nodes. Eq. (2) can be written more compactly as the interpolation

$$u = \sum_{i=1}^{3} h_i \mathcal{P}_i^p \tag{4}$$

Hence, instead of using the traditional interpolation $h_i\, u_i$, we now use the interpolation $h_i\, \mathcal{P}_i^p$, where $\mathcal{P}_i^p$ contains the usual nodal variable u_i plus the cover bases times additional nodal variables, as in

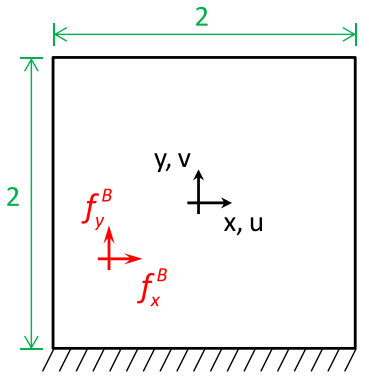

In-plane displacements (with $k = 5$)

$$u = (1-x^2)^2(1-y^2)^2 e^{ky}\cos(kx)$$

$$v = (1-x^2)^2(1-y^2)^2 e^{ky}\sin(kx)$$

Corresponding body forces

$$f_x^B = -\left(\frac{\partial \tau_{xx}}{\partial x} + \frac{\partial \tau_{xy}}{\partial y}\right), \quad f_y^B = -\left(\frac{\partial \tau_{yy}}{\partial y} + \frac{\partial \tau_{yx}}{\partial x}\right)$$

Fig. 2. Ad hoc in-plane analysis, plane stress conditions with $E = 2e5$ and $\nu = 0.3$.

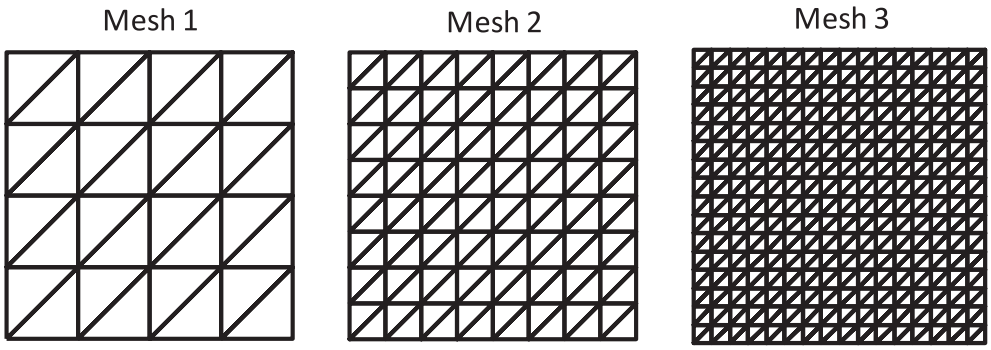

Fig. 3. Sequence of meshes used for the analysis of the ad hoc test problem.

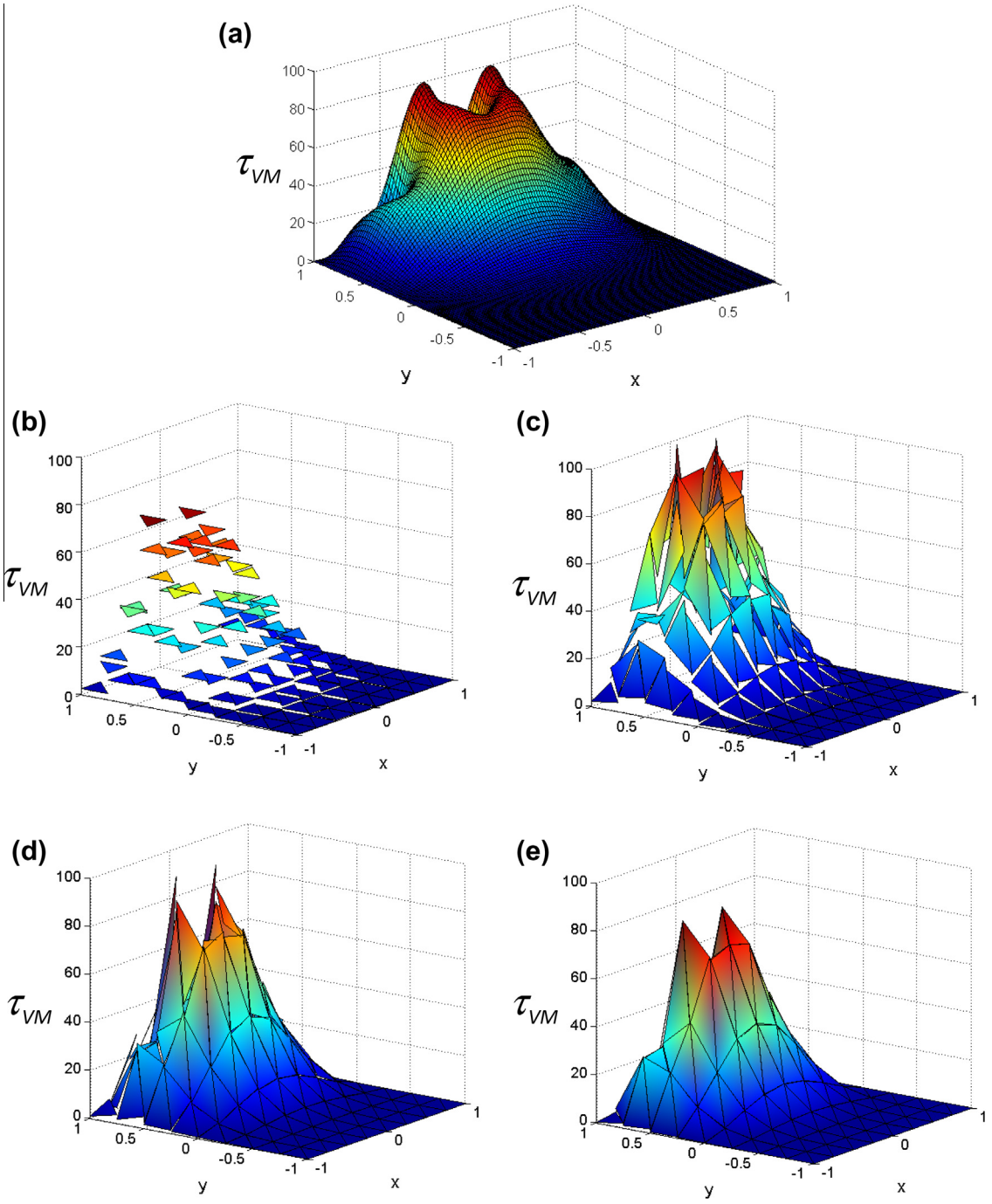

Fig. 4. Plots of von Mises stress field: (a) exact solution, and solutions with Mesh 2 using (b) linear element, (c) linear covers, (d) quadratic covers, and (e) cubic covers.

Eq. (1). Since the traditional interpolation functions h_i give displacement compatibility between elements, Eq. (4) shows that this compatibility is also preserved in the cover scheme for any order of covers applied at the nodes. Here it is important to note that the order p can of course vary from node to node, and if $p = 0$, there is no interpolation cover used for that node.

Indeed, our objective in this paper is to propose a scheme for choosing the order of the interpolation covers to reach an improvement in solution accuracy at a reasonable cost.

Some important features of the basic scheme were discussed in Ref. [1], and specifically how to ensure a positive definite coefficient matrix by applying the Dirichlet boundary conditions as usual and without covers at the nodes on such boundaries. We will proceed in this way throughout the solutions given below.

We should note that the proposed scheme only enriches the interpolation for the solution variable u, and only to some degree (given by the maximum cover order used). Furthermore, the scheme does not enrich the interpolation of the geometry, for which always only the original mesh of low-order elements is employed. Hence, there are limitations as to how much the solution accuracy can be increased, in particular when there are complex curved boundaries (of course, the geometry interpolation could also be enriched in a further development of the scheme, see Concluding Remarks). Indeed, we will illustrate in the example

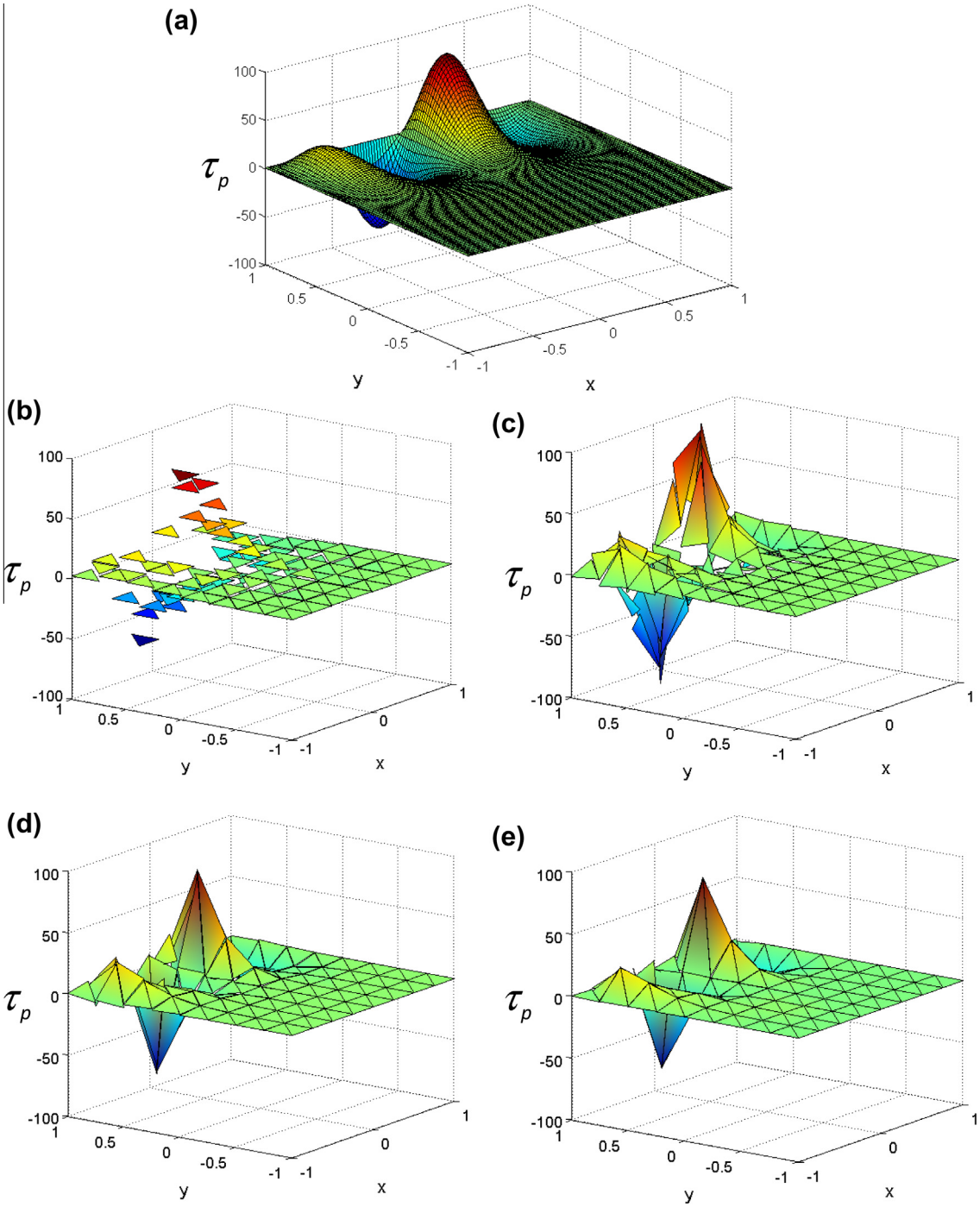

Fig. 5. Plots of pressure field: (a) exact solution, and solutions with Mesh 2 using (b) linear element, (c) linear covers, (d) quadratic covers, and (e) cubic covers (where τ_p denotes pressure).

solutions, see Section 4, that the underlying mesh should already be a reasonable mesh giving already, overall, a reasonably accurate solution. The enrichment scheme is then used to only "somewhat" increase the accuracy of the displacement and stress predictions.

3. The procedure to improve the displacement and stress predictions

Our goal is to establish an algorithm that determines appropriate cover orders to improve the solution accuracy when a reasonable solution has already been obtained but that solution is judged to be not of sufficient accuracy, in particular regarding the stress prediction. The complete solution process is as follows:

Assume that we have performed an analysis as usual – we have chosen a reasonable finite element mesh and obtained a solution, where in this paper we only consider meshes of 3-node triangular and 4-node tetrahedral elements in 2D and 3D analyses, respectively.

The solution results are next improved as follows. A simple error indicator is employed to identify in which regions the relative errors are larger than a prescribed (relative) allowable value. Then, corresponding to the level of error, either no interpolation cover, linear, quadratic or cubic interpolation covers are applied to obtain

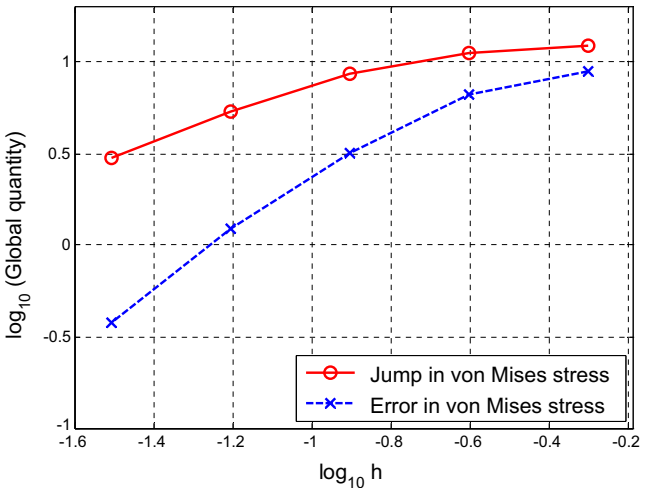

Fig. 6. Ad hoc problem: convergence of the global stress jumps and errors in the von Mises stress field.

a more accurate solution. If the solution is considered to be still not sufficiently accurate, a next solution improvement is obtained by applying more and higher-order covers, and the process can be repeated until the estimated error is smaller than the allowable error value or until the highest order of interpolation cover (here selected to be a cubic cover) has been applied to all nodes.

Since the most accurate solution would usually be obtained with the cubic interpolation covers applied to all nodes, it is clear that, for a given mesh, there is a limit to the solution accuracy that can be obtained. We illustrate this fact below. Hence it is important that a reasonable initial (original) mesh is used and that the required solution accuracy is not too far from the accuracy obtained with that mesh.

Of course, the traditional way to proceed is to remesh or use higher-order elements, mostly only in certain regions, when a better solution accuracy is needed. Depending on the analysis pursued, the cover scheme may use less or more computational time than using the traditional approach, but the method has the advantage that no new elements or nodes are created, no new nodal locations are used, and no special transition elements between lower and higher-order elements are introduced. Hence, the use of the scheme requires significantly less human effort in preparing the input data for reaching a more accurate solution.

In order to establish an effective adaptive cover scheme, we need to estimate the local solution quality at the mesh nodes and determine which orders of covers should be applied. Hence, a reliable indicator of the solution error is needed. Various mathematically formulated 'a posteriori' error estimation methods have been proposed over many years to evaluate the overall quality of a finite element solution by establishing error measures of global energies and of local quantities [6]. However, so far no estimation scheme is available that is proven to always give an 'effective upper bound' to the actual error (in the sense that the estimate is always only a little larger than the actual error), the scheme is 'general' (in the sense that it is applicable to all problems), and the scheme is 'computationally efficient' (in the sense that the error is calculated with much less computational effort than simply solving the problem using an extremely fine mesh). For this reason, mathematically formulated error measures are hardly used in engineering practice. The basic difficulty is of course that an error to the exact solution is to be estimated when the exact solution is unknown. In nonlinear analyses, an additional difficulty is that there may be multiple solutions.

Instead of trying to measure the solution error, another approach is to use element measures to establish effective elements. Then the element sizes are selected such that the change in a specific solution quantity (e.g. the gradient of a field) is about constant for each element. In this case, a sequence of meshes is used until the solutions hardly change, see for example Ref. [7]. However, such approaches do not directly lend themselves for use in the cover scheme that we envisage here, since we need an error indicator.

For the scheme to be proposed here, also a global energy-based error measure is not of value because it cannot be used to measure the local solution accuracy, and we need to focus on local error measures. An explicit *local* error indicator η_m for element m is given by [6]

$$\eta_m^2 = c_1 h^2 \|\mathbf{R}\|^2_{\mathbb{L}^2(\mathbb{m})} + c_2 h \|\mathbf{J}\|^2_{\mathbb{L}^2(\partial\mathbb{m})} \tag{5}$$

where $\mathbf{R}$ denotes the interior element residual calculated from the differential equilibrium equations, $\mathbf{J}$ denotes the jump in the stress across the element edges, and h is the element size. In Eq. (5), the values of the constants c_1 and c_2 are generally unknown, since these depend on the exact solution which is not known, and would need to be estimated. However, the estimator shows that we have second order convergence for the residual $\mathbf{R}$ norm squared and first order convergence for the stress jump $\mathbf{J}$ norm squared with respect to h. Assuming that the constants c_1 and c_2 have about the same magnitude, and a reasonably fine mesh is used, we can neglect the element residual and focus on the element stress jumps. This approach indeed was used in the construction of the stress band plots to indicate solution errors [4,6,8].

The requirements we would like to fulfill with the selected error indicator are:

- The indicator should be simple and computationally efficient; that is, inexpensive to compute when measured on the total computational time used for the solution.
- The indicator should asymptotically converge as the actual error converges.
- The indicator should directly tell where covers are best applied and what cover orders are best used, and that for a large range of problems.
- No parameter should be used in the definition of the error indicator.

Based on these requirements, we do not use Eq. (5) but instead calculate the largest stress jump for a scalar stress quantity of interest (say τ) as

$$J_i^\tau := \max_{m\in m_c(i)} \left\{\tau_i^{h(m)}\right\} - \min_{m\in m_c(i)} \left\{\tau_i^{h(m)}\right\} \tag{6}$$

where $\tau_i^{h(m)}$ denotes the nodal stress evaluated at node i for element m and we search over all elements connected to the node i. Hence $m_c(i)$ denotes the set of elements participating in cover C_i, i.e.

$$m_c(i) := \{m : C_i \cap \mathcal{E}^m \neq \emptyset\} \tag{7}$$

Note that the jump J_i^τ is always positive.

To study the behavior of the stress jump values when covers are applied and when compared to the actual error at the nodes, we consider the ad hoc problem given in Fig. 2 (see also Refs. [1,4]).

The figure gives the domain considered, and the exact displacements and corresponding body forces. In the testing of finite element schemes, we apply the body forces, calculate the displacement and stress results and compare these with the exact values.

Fig. 3 shows a sequence of meshes used for the analyses. The finer meshes (Mesh 4, Mesh 5, etc.) can be directly inferred from the patterns shown. Figs. 4 and 5 show the calculated von Mises stress and the pressure when using Mesh 2, as covers are applied.

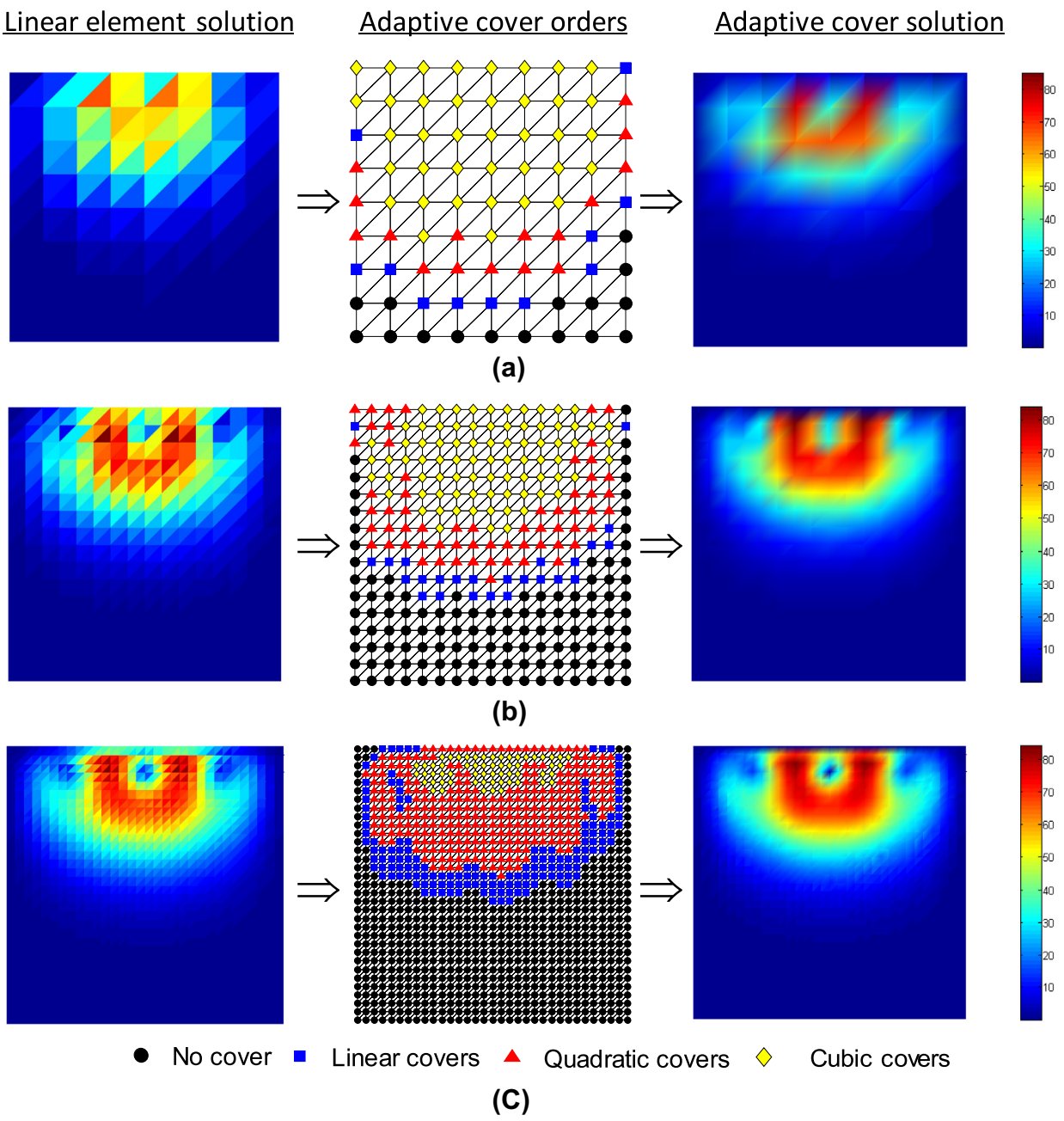

Fig. 7. Von Mises stress prediction by the proposed adaptive scheme using (a) Mesh 2, (b) Mesh 3, and (c) Mesh 4.

Table 1
Comparison of percentage errors in 1 and 2-norms for von Mises stress and pressure. Nodal values are used. The maximum desirable error is 2%.

Mesh	Relative errors in 1-norm				Relative errors in 2-norm			
	$\|\underline{\varepsilon}^{\tau_{VM}}\|_1/\|\underline{\tau}_{VM}\|_1$		$\|\underline{\varepsilon}^{\tau_p}\|_1/\|\underline{\tau}_p\|_1$		$\|\underline{\varepsilon}^{\tau_{VM}}\|_2/\|\underline{\tau}_{VM}\|_2$		$\|\underline{\varepsilon}^{\tau_p}\|_2/\|\underline{\tau}_p\|_2$	
	Linear element	Adaptive covers	Linear element	Adaptive covers	Linear element	Adaptive covers	Linear element	Adaptive covers
2	51.0	5.1	81.0	3.5	59.3	8.4	80.0	3.1
3	22.2	0.9	33.9	0.7	36.4	1.2	44.7	0.7
4	8.2	0.9	11.0	0.7	18.6	1.0	20.5	0.6

The figures illustrate how the stress jumps decrease and in fact almost disappear as the order of covers is increased.

Fig. 6 shows the convergence of the globally-representative (or global, for short) nodal stress jumps and actual errors in the calculated von Mises stress, where the global quantities are defined as

$$\bar{J}^{\tau} = \frac{1}{N}\sum_{i=1}^{N} J_i^{\tau}, \quad \bar{\varepsilon}^{\tau} = \frac{1}{N}\sum_{i=1}^{N} \varepsilon_i^{\tau} \tag{8}$$

N denotes the number of nodes used in the mesh, and we considered the magnitude of errors, i.e. $\varepsilon_i^{\tau} = \left|\tau_i - \tau_i^h\right|$ using the exact stress

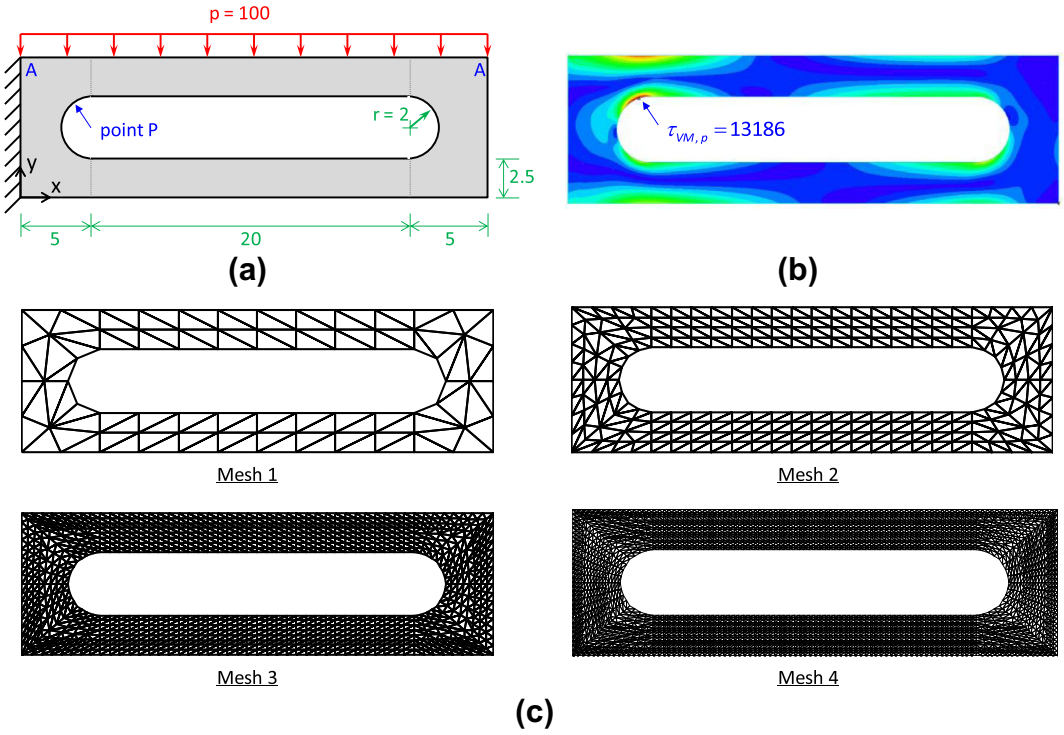

Fig. 8. Two-dimensional tool jig problem, (a) problem description, $E = 72e9$, $\nu = 0.3$, (b) reference von Mises stress plot, and (c) meshes used in the cover solutions and the higher-order 6-node element solutions.

τ_i and the averaged computed stress τ_i^h at node i. For the results in Fig. 6, simply the mesh refinements (as given in Fig. 3) are used without covers.

As seen in the figure, both global quantities converge, but the actual errors are smaller and converge faster than the stress jumps. The observed convergence orders in this problem solution are approximately

$$\begin{cases} \bar{J}^\tau \sim \mathcal{O}(h^{\alpha_J}) \\ \bar{\varepsilon}^\tau \sim \mathcal{O}(h^{\alpha_\varepsilon}) \end{cases} \quad \text{with} \quad \alpha_J = 0.8,\ \alpha_\varepsilon = 1.6 \tag{9}$$

While we have no mathematical proof that the actual errors are always smaller than the stress jumps as defined in Eqs. (6) and (8), we have observed such behavior in all our analyses and it is a reasonable result because we establish in Eq. (6) the *maximum* stress jump at the node.

Based on the given theoretical and numerical observations, we use J_i^τ in establishing the indicator that shall tell what interpolation cover to apply to node i. Let

$$\mathcal{M}_i^\tau = \frac{J_i^\tau}{\gamma_e \tau_{\text{mean}}} (h/L_c)^\beta \tag{10}$$

where τ_{mean} is the calculated mean stress (using absolute values) over the complete domain, γ_e is a specified *small* constant so that $\gamma_e \tau_{\text{mean}}$ is an accuracy tolerance for the jump, L_c is a characteristic length, and $(h/L_c)^\beta$ is used to have in $\mathcal{M}_i^\tau$ an order of convergence close to the order of convergence of the actual error. Here, the value of β needs to be chosen by the user. Relating the relative element size h/L_c in two- and three-dimensional analyses to the number of nodes in the mesh, we can use $h/L_c \sim N^{-1/2}$ and $h/L_c \sim N^{-1/3}$, respectively, so that the indicator $\mathcal{M}_i^\tau$ is a dimensionless value independent of domain size as well as the material data.

To choose the order of a cover $p(i)$ at a node i, we then use the following scheme:

$$p(i) = \begin{cases} 0 & \text{if} \quad \mathcal{M}_i^\tau < \gamma_0 \\ 1 & \text{if} \quad \gamma_0 \leqslant \mathcal{M}_i^\tau < \gamma_1 \\ 2 & \text{if} \quad \gamma_1 \leqslant \mathcal{M}_i^\tau < \gamma_2 \\ 3 & \text{if} \quad \gamma_2 \leqslant \mathcal{M}_i^\tau \end{cases} \tag{11}$$

where γ_k, $k = 0, 1, 2$ denote 'adaptivity threshold constants' to be set by the user.

With this adaptivity indicator any stress quantity of interest can be used, but in this work, we employ jumps of the von Mises stress and the pressure so that, both, the deviatoric stress and the pressure enter in the selection of the cover. Usually we use $\mathcal{M}_i^\tau = (\mathcal{M}_i^{\tau_{VM}} + \mathcal{M}_i^{\tau_p})/2$, but it is important to realize that the value corresponding to one stress may be much larger than for the other stress. In such a case, it may be necessary to apply Eq. (11) separately for the von Mises stress and pressure with different constants, and then use the highest cover value obtained for the node.

As mentioned above, the user needs to choose β and the constants γ_k, and some guidelines are here useful. Considering the convergence in the ad hoc example, as a model problem with $L_c = 1$, we first use the sequence of meshes shown in Fig. 3 to obtain the mean values (averaged over all nodes) of stress jumps using the linear elements with no covers. Then we obtain the solutions and curves of 'actual errors' using no covers, and linear and quadratic covers on the same meshes with the covers applied at all nodes. The value of β for a cover is chosen to turn the convergence curve slope of the 'no cover solutions measuring stress jumps' downwards to the slopes of the convergence curves of the above-mentioned 'actual errors' and the adaptivity constants are obtained based on shifting the curve of the 'no cover solutions measuring stress jumps' downwards to the convergence curves of the 'actual errors'. To obtain those shifts the solutions at a reasonable refinement are used. The measured respective values, thus obtained, are approximately $\beta = 0.8$, 1.3 and 2, and $\gamma_0 = 0.4$, $\gamma_1 = 0.9$ and $\gamma_2 = 3.6$, using $L_c = 1$. Of course, these values cannot have general applicability

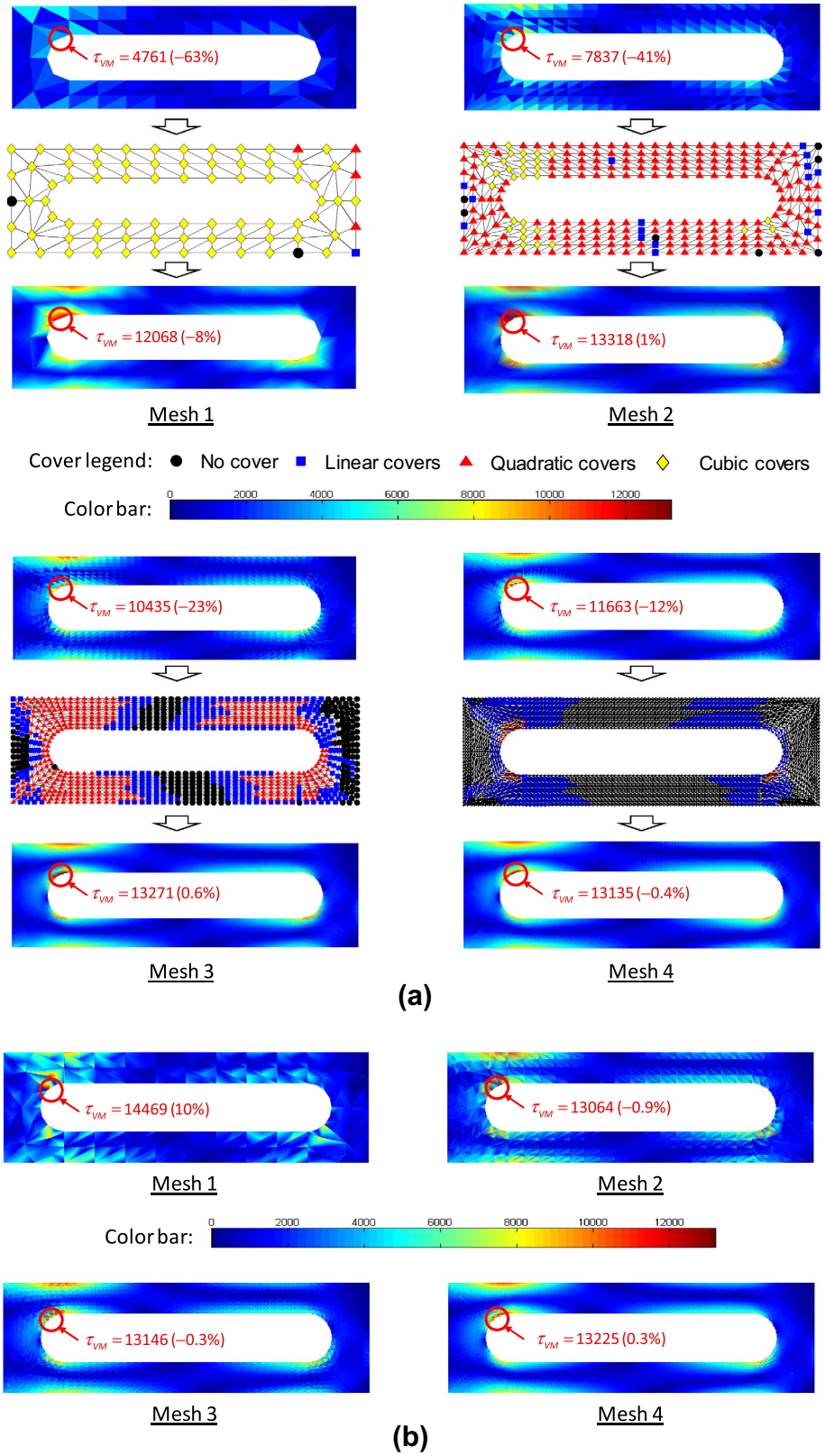

Fig. 9. Von Mises stress results: (a) enriching solutions using the proposed adaptive interpolation, and (b) solutions using the 6-node elements.

but for this ad hoc problem approximately optimal convergence rates are obtained, see Ref. [1]. Hence when using well-constructed meshes in the solution of other problems, these constants determined in the solution of the ad hoc problem might be used in the first instance when no better values are available, and we shall do so in the example solutions of Section 4.

The above scheme and results are rather simple, and different threshold slope adjustments and threshold constants should

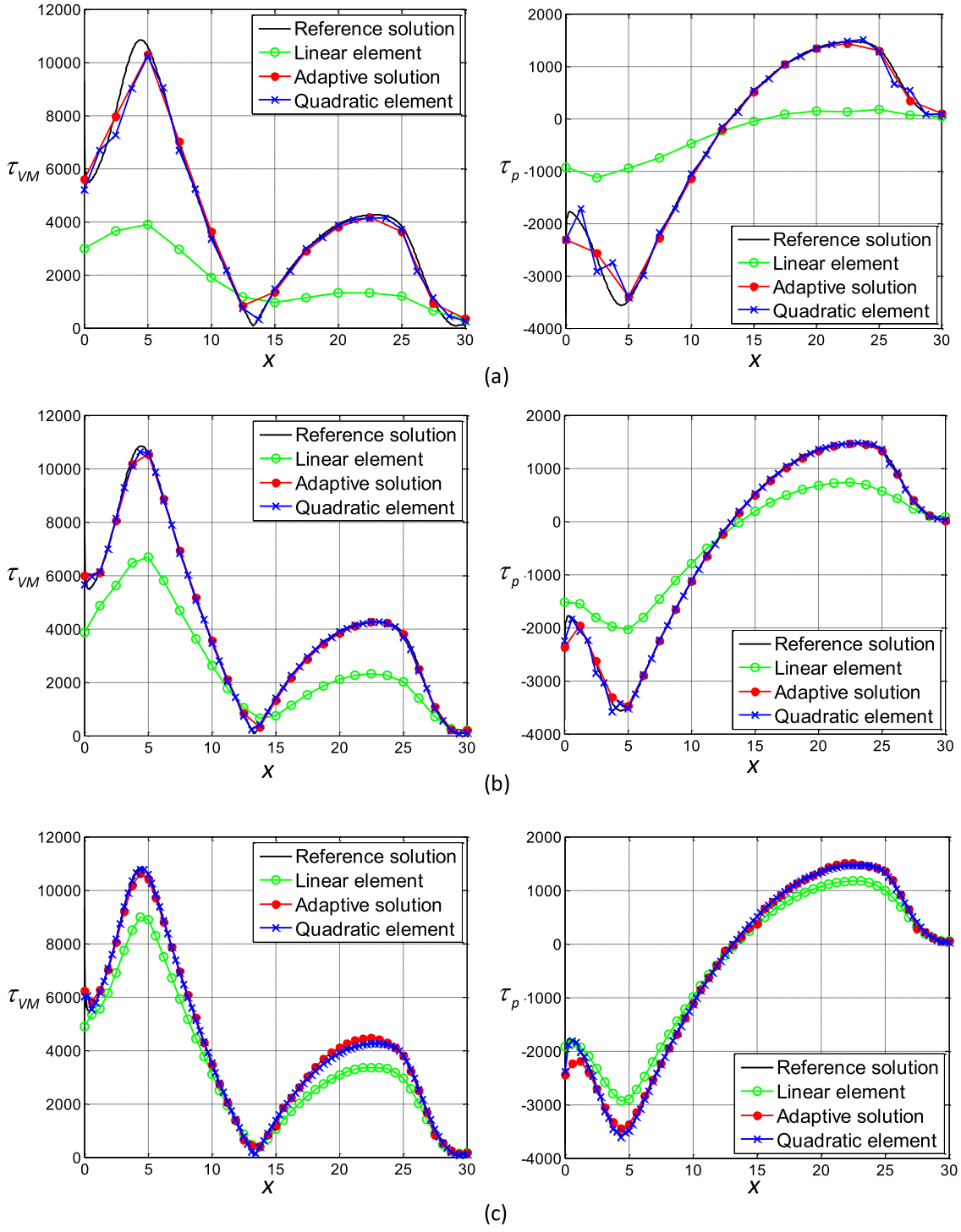

Fig. 10. Plots of (left) von Mises stress and (right) pressure along the evaluation line AA, see Fig. 8(a), using (a) Mesh 1, (b) Mesh 2, (c) Mesh 3.

probably be used in regions of stress concentrations, edges and corners, since the ad hoc problem contains no stress singularities.

As an illustration, Fig. 7 shows results obtained with the scheme and the above given constants for the ad hoc problem using Meshes 2–4. As seen, the order of covers is automatically determined to improve the accuracy, and the required enrichment naturally decreases as the mesh is refined. Table 1 gives some quantitative comparisons of the solution errors in the 1- and 2-norms [4]. As shown in the figure and the table, provided the mesh is fine enough, like Mesh 3, the required solution accuracy is reached by predominantly using high-order covers, while if the mesh is not sufficiently fine, like Mesh 2, the required solution accuracy is not reached even though the highest order covers are used almost over the complete domain. The Mesh 2 results are not sufficiently accurate although the stress jumps in Figs. 4 and 5 can hardly be seen. Therefore, it is important to use a reasonably fine mesh in the complete solution process, but that will generally be the case in engineering practice.

Table 2
Computational results for the two-dimensional tool jig problem.

		Linear element	Adaptive scheme	Quadratic element
Mesh 1				
τ_{VM} at point P (error in%)		4761 (−63%)	12068 (−8%)	14469 (10%)
DOFs (m_K)		150 (13)	1436 (137)	510 (69)
Computation time (s)		0.0	0.6	0.0
Cond ($\underline{K}$)	Usual bases	1.5*e*5	2.8e10	1.3*e*4
	Normalized bases		2.1*e*9	
Mesh 2				
τ_{VM} at point P (error in%)		7837 (−41%)	13318 (1%)	13064 (−0.9%)
DOFs (m_K)		526 (26)	3262 (179)	1918 (197)
Computation time (s)		0.1	1.3	0.6
Cond ($\underline{K}$)	Usual bases	1.1*e*6	6.2*e*9	7.6*e*4
	Normalized bases		7.8e7	
Mesh 3				
τ_{VM} at point P (error in%)		10435 (−23%)	13271 (0.6%)	13146 (−0.3%)
DOFs (m_K)		1950 (57)	7954 (272)	7422 (645)
Computation time (s)		0.3	3.5	14.2
Cond ($\underline{K}$)	Usual bases	6.7*e*6	1.9*e*8	3.6*e*5
	Normalized bases		2.3*e*7	
Mesh 4				
τ_{VM} at point P (error in%)		11663 (−12%)	13135 (−0.4%)	13225 (0.3%)
DOFs (m_K)		6654 (121)	11818 (278)	25918 (2419)
Computation time (s)		1.5	6.0	666.4
Cond ($\underline{K}$)	Usual bases	2.5*e*7	4.3*e*8	1.3*e*6
	Normalized bases		7.1*e*7	

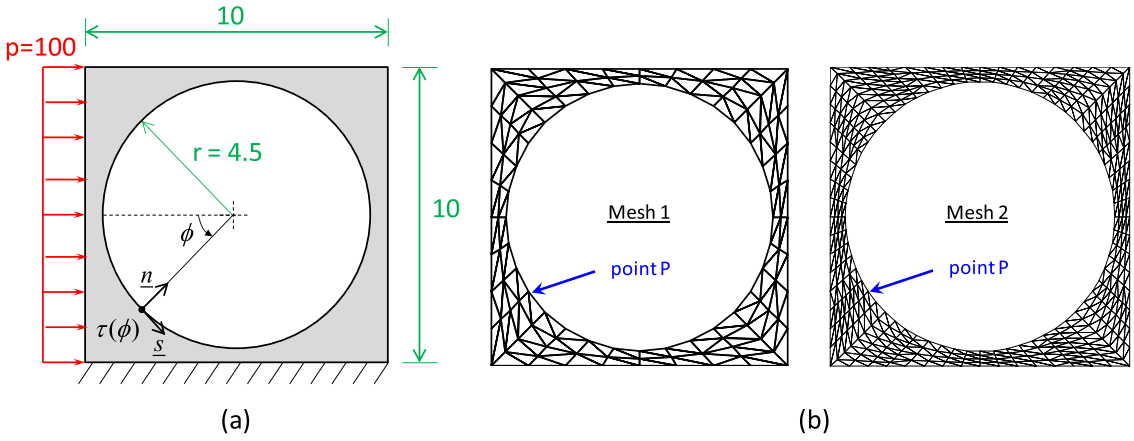

Fig. 11. Plate with a hole: (a) problem description, $E = 72e9$, $\nu = 0$, and (b) meshes used.

4. Illustrative examples

In this section we give various solutions obtained using the scheme presented above. We consider two-dimensional and three-dimensional solutions, of course, obtained using the constant strain 3-node triangular and 4-node tetrahedral elements, respectively. In each case we use the data for steering the scheme, identified and used in the solution of the ad hoc problem in Section 3. To study the computational effectiveness we also compare the solution times used to reach a specified accuracy when employing the automatic enrichment procedure compared to simply using higher-order elements, albeit each time for the complete domain. All solutions were obtained using the program STAP, see Ref. [4], in which the enrichment scheme has been implemented with the standard low-order elements, using a PC machine with a single core. In the following we report solution times for which only relative values are important.

4.1. Two-dimensional simulations

With the above objectives, we present in this section some two-dimensional analyses. In each analysis, we compare the numbers of degrees of freedom (DOFs), the mean half-bandwidths m_K, the condition numbers of the global system matrices, and the solution times used for the analyses.

4.1.1. 2D tool jig problem

We first consider a two-dimensional tool jig problem subjected to a constant pressure load as shown in Fig. 8. This problem was already solved in Ref. [1], and also considered in Ref. [9]. Since the analytical solution is not available, we use a very fine mesh of 40,000 9-node elements leading to 323,200 degrees of freedom to obtain a reference solution. Using the proposed adaptive scheme and 6-node quadratic elements, we compare the solution accuracies and computational costs using Meshes 1–4. The stress results are compared at the evaluation point P and along the line AA shown in Fig. 8(a).

Fig. 9(a) shows how the adaptive interpolation performed to increase the accuracy in the von Mises stress. As seen in the figure, the solutions are greatly improved by using the interpolation covers. It should be noted that the adaptive scheme appropriately distributes cover orders for the given meshes – if the mesh is very coarse, like Mesh 1, then higher-order covers are mainly used, while if the mesh is fine, like Mesh 4, then low-order interpolation

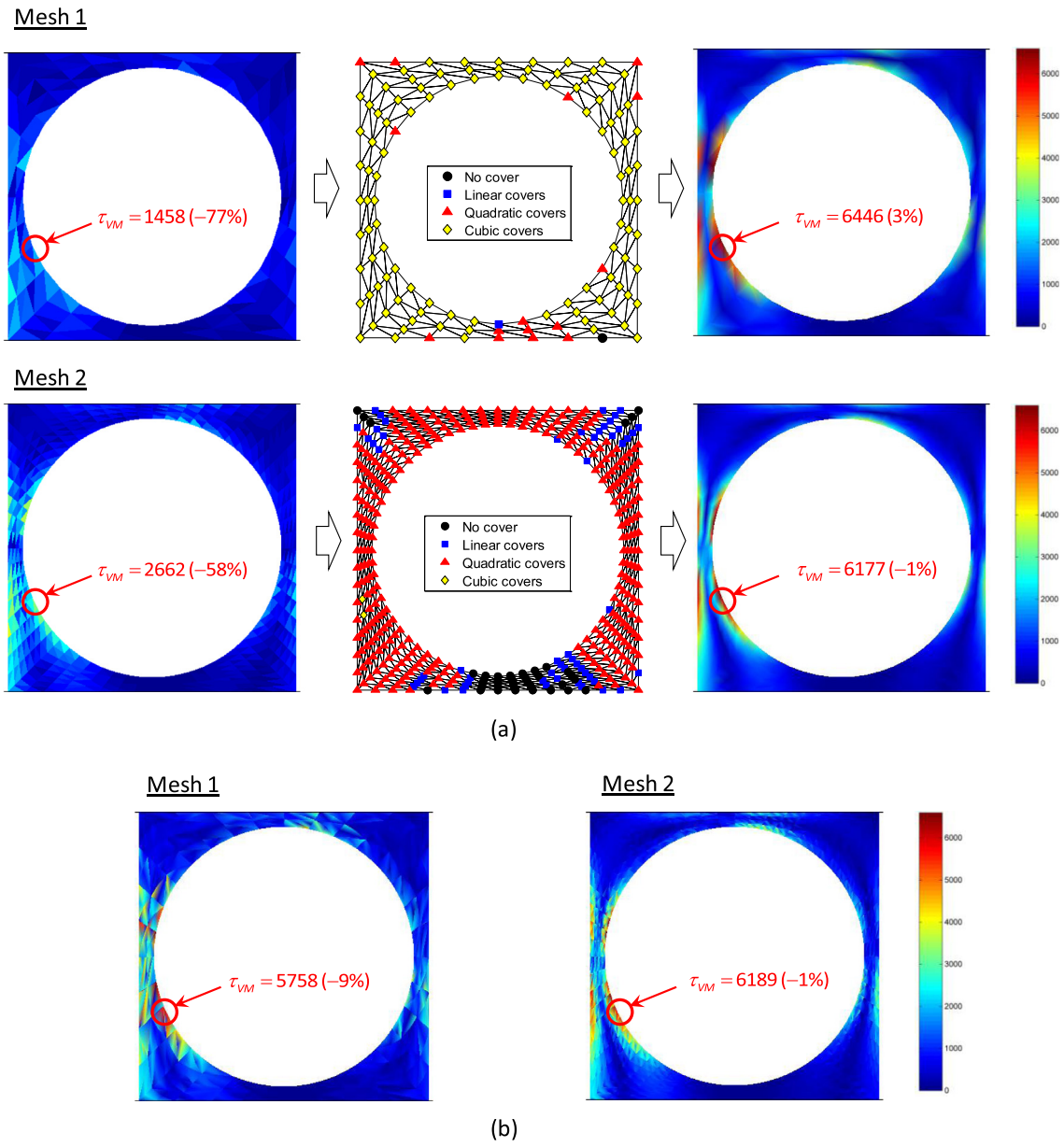

Fig. 12. Plots of calculated von Mises stress: (a) using the adaptive scheme, and (b) using quadratic elements.

Table 3
Computational results for the plate with a hole problem.

		Linear element	Adaptive scheme	Quadratic element
Mesh 1				
τ_{VM} at point P (error in%)		1458 (−77%)	6446 (3%)	5758 (−9%)
DOFs (m_K)		222 (20)	2118 (198)	798 (85)
Computation time (s)		0.0	1.2	0.1
Cond ($\underline{K}$)	Usual bases	1.0*e*5	1.1*e*11	4.1*e*4
	Normalized bases		2.0*e*10	
Mesh 2				
τ_{VM} at point P (error in%)		2662 (−58%)	6177 (−1%)	6189 (−1%)
DOFs (m_K)		830 (47)	4390 (262)	3134 (243)
Computation time (s)		0.1	2.7	1.1
Cond ($\underline{K}$)	Usual bases	8.1*e*5	1.2*e*9	1.6*e*8
	Normalized bases		8.8*e*6	

covers become predominant. Fig. 9(b) shows the analysis results using the 6-node quadratic element. As seen, the von Mises stress at the evaluation point P converges similarly when using the quadratic element and the adaptive interpolations. Indeed, as shown in Fig. 10, which gives the plots of von Mises stress and pressure along the specified line AA, the overall stress results are

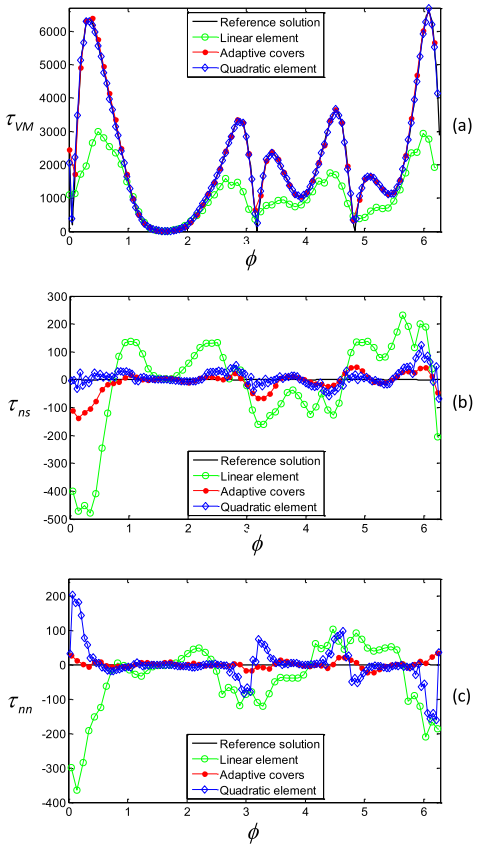

Fig. 13. Stress distributions along the perimeter of the hole: (a) von Mises stress, (b) shear stress, and (c) normal stress; note the different scales used.

excellent using Meshes 2 and 3 with the adaptive scheme. Also, the pressure results obtained using Meshes 1 and 2 are slightly better with the adaptive scheme than when using the quadratic element.

Table 2 gives a comparison of computational aspects, including the solution times. For Meshes 1 and 2, the solution times are very small. Then for Meshes 3 and 4 the times are considerably larger using the quadratic element than applying interpolation covers with about the same accuracy reached for the von Mises stress at point P. In fact, if the required solution accuracy for the stress at point P is a 2% error, then Mesh 2 is sufficient, and Meshes 3 and 4 are not needed. On the other hand, the use of the interpolation covers improves a (very) little the solution accuracy using Meshes 3 and 4 while the computation time does not grow much with increasing mesh density; hence, the analyst has more flexibility. The condition numbers are reasonable for all coefficient matrices used, and the normalization of the cover degrees of freedom results into only small improvements (with $\widehat{h}$ set to the average element size, in all problem solutions).

4.1.2. Plate with a hole

In this analysis we consider a plate with a large circular hole in its center subjected to a pressure load, as shown in Fig. 11. We seek the von Mises stress at point P and the stresses along the perimeter of the hole using the standard 3-node linear element, with and without covers, and using the 6-node quadratic element. Meshes 1 and 2 shown in the figure are used. The reference solution is obtained using a fine mesh of 8,192 9-node quadrilateral elements, which leads to 66,560 degrees of freedom.

Fig. 12 shows the calculated von Mises stress band plots. The adaptive scheme with Mesh 1 uses mostly cubic covers, while with Mesh 2 a significant number of lower order covers are used. Assuming that a solution with no more than 3% error for the von Mises stress at point P is sought, the quadratic element (using this

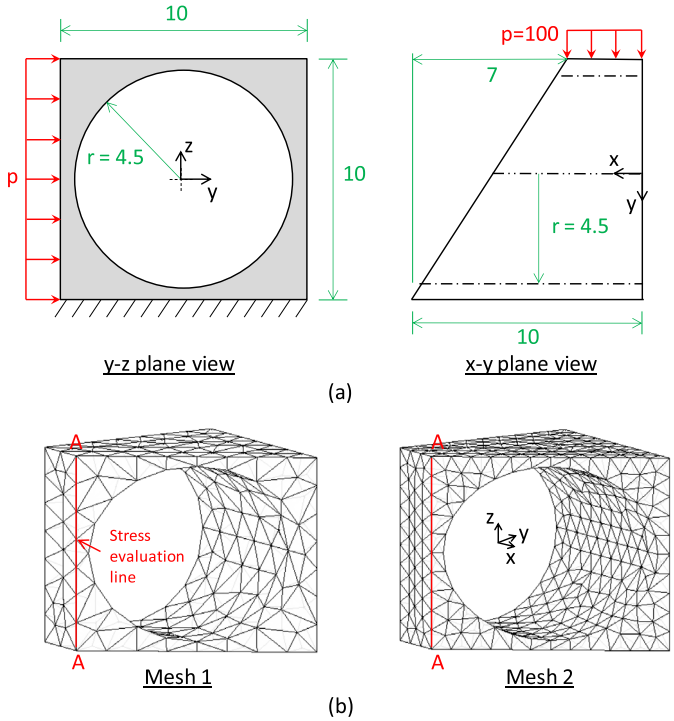

Fig. 14. Slantly-cut body with a round tunnel, (a) problem description, $E = 72e9$, $\nu = 0.3$, and (b) tetrahedral element meshes used.

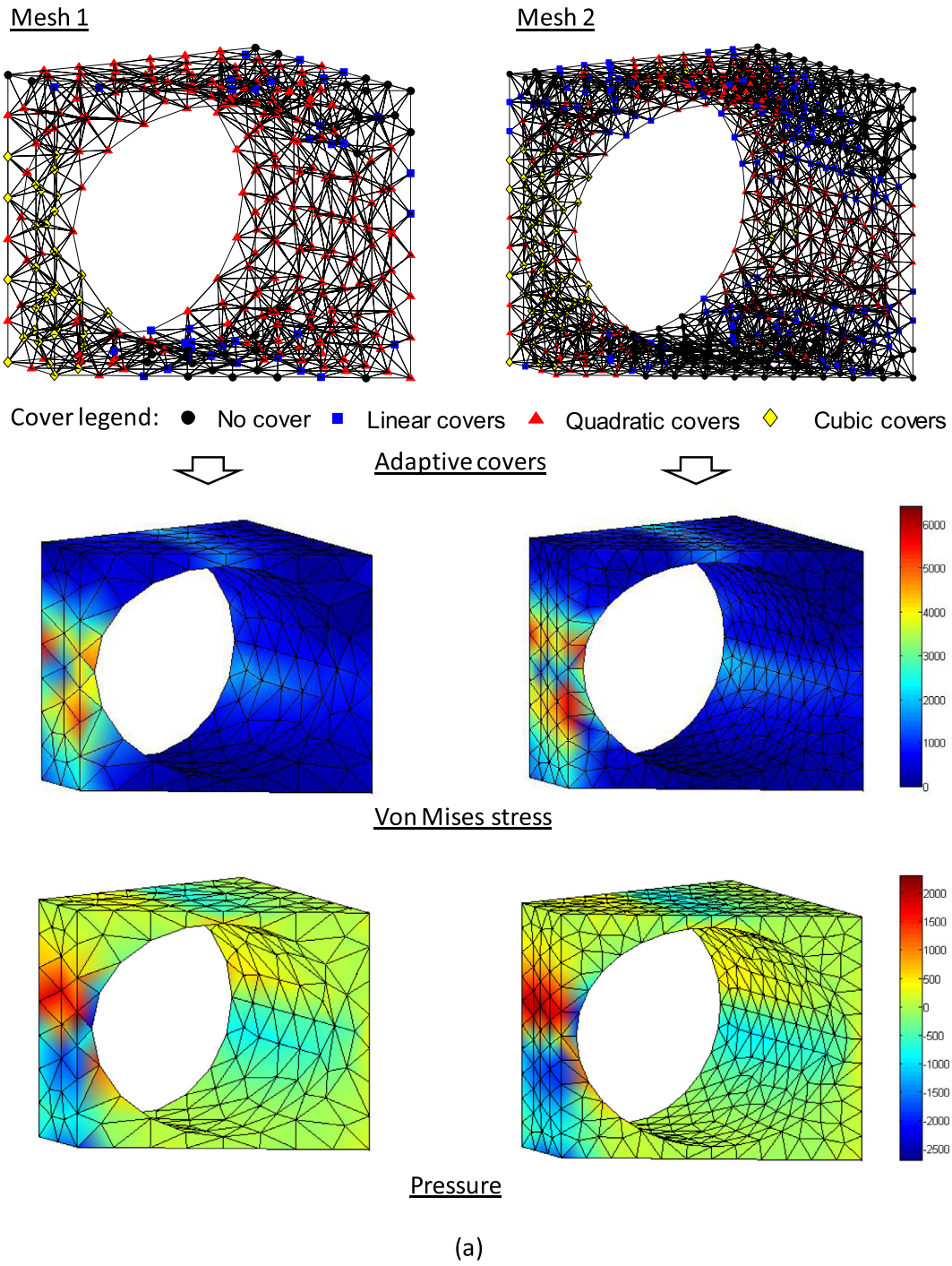

Fig. 15. Von Mises stress and pressure calculation results of the slantly-cut body problem, (a) adaptive scheme solutions, and (b) quadratic element solutions.

element for the complete domain) requires Mesh 2, while this accuracy is reached with both meshes using the cover scheme, see Table 3. The computational times used with the adaptive scheme are greater than those using the quadratic element, but still small, so that in practice the solution times using the covers are acceptable. As with the solutions in Section 4.1.1, the condition numbers are reasonable and improved by the normalization of the cover degrees of freedom.

Physical equilibrium requires $\tau_{nn} = \tau_{ns} = 0$ along the perimeter of the hole, but the numerical solutions show significant errors if the mesh is not fine enough. Fig. 13 shows the calculated stress distributions using Mesh 2. The solution is improved using covers, especially for the normal stress.

4.2. Three-dimensional simulations

In this section we consider solutions of two three-dimensional problems. While the use of linear covers can be more efficient than the use of quadratic elements, the use of three-dimensional covers higher than linear yields a rapidly increasing number of unknowns and the solution times can increase significantly; however, the same of course also holds when using traditional higher-order elements.

4.2.1. Slantly-cut body

We consider a body cut slantly with a round hole subjected to a constant pressure load as shown in Fig. 14, where also the two

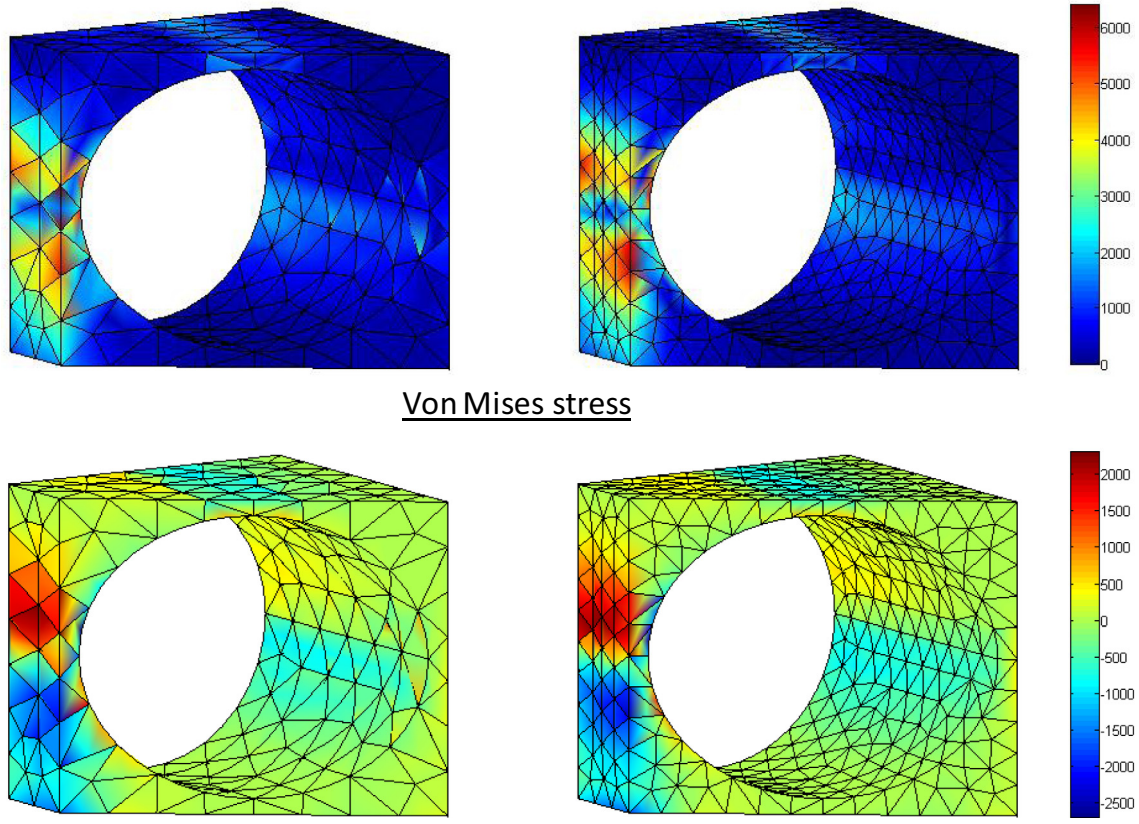

Fig. 15 (*continued*)

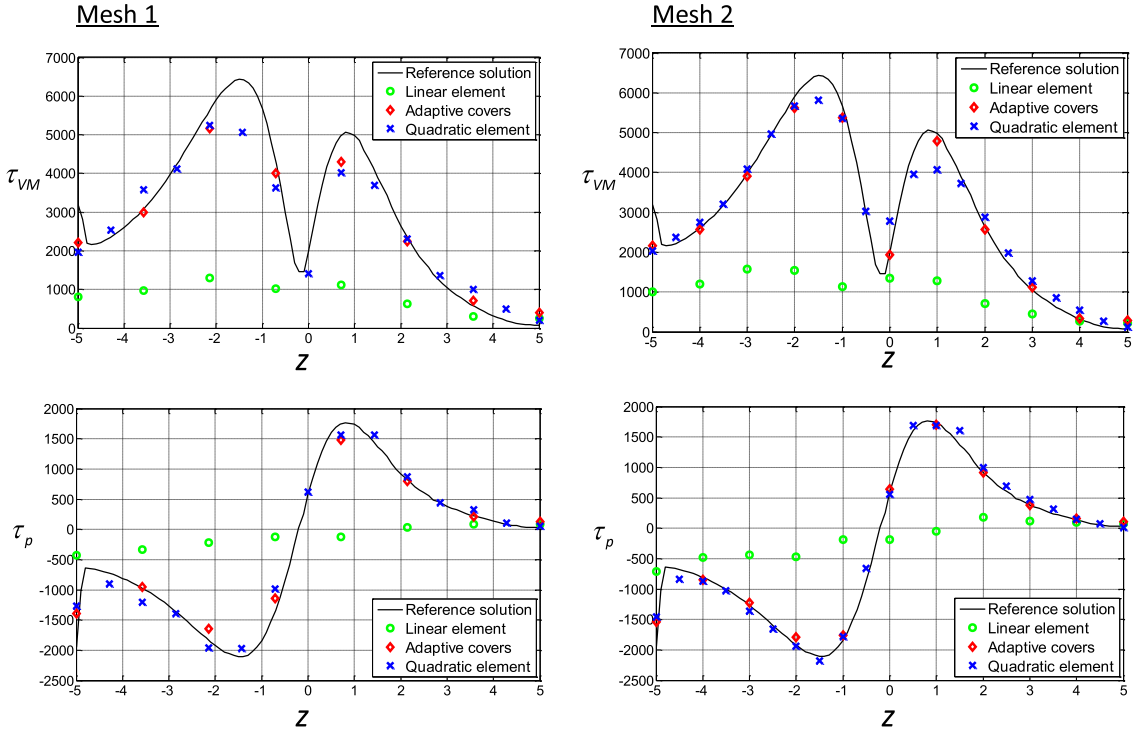

Fig. 16. Von Mises stress and pressure plots along the evaluation line AA (τ_p denotes pressure).

Table 4
Computational results for the slantly-cut body problem.

	Mesh 1		Mesh 2	
	Adaptive scheme	Quadratic element	Adaptive scheme	Quadratic element
DOFs (m_K)	7575 (2356)	4719 (2144)	14280 (4353)	11310 (5113)
Computation time (s)	146	73	881	994
Cond ($\underline{K}$)	1.8*e*7	1.8*e*8	2.2*e*11	8.5*e*11

meshes used and the stress evaluation line AA ($x = 3$, $y = -5$) are shown. The reference solution was obtained using a very fine mesh of 163,166 10-node tetrahedral elements, leading to 738,129 degrees of freedom.

Figs. 15 and 16 show the von Mises stress and pressure results obtained using the proposed adaptive scheme and quadratic elements. As seen in Fig. 16, the adaptive scheme provides good accuracy using Mesh 2, while the quadratic element mesh does not provide sufficient accuracy in some areas. We also note that the adaptive scheme uses more degrees of freedom but less solution time for Mesh 2, see Table 4. With the quadratic elements, a finer mesh is needed to obtain an accurate result, but then the solution time would significantly increase. The computation times given in Table 4 show the effectiveness of the method since the adaptive scheme yields for Mesh 2 a smaller half-bandwidth.

4.2.2. Three-dimensional tool jig

We consider a three-dimensional tool jig subjected to the pressure load shown in Fig. 17. In this example, we employ three different mesh patterns, Mesh A1, Mesh A2 and Mesh B1. The reference solution was obtained using a mesh of 16,000 27-node brick elements leading to 423,360 degrees of freedom.

We use Mesh A1 and Mesh A2 for the adaptive scheme and Mesh B1 for the quadratic element solution. For a result comparison, a stress evaluation window is defined in Fig. 17.

Fig. 18 shows the band plots of calculated von Mises stress and pressure. Note that the colormap for pressure does not span the entire range of pressure variation in order to be able to see some details. Fig. 19 shows the stress results on the stress evaluation window (the rectangle ABCD), in which averaged stresses at nodal points are employed for the plots (hence the stresses are smooth). According to the figures and Table 5, the solution obtained using Mesh A2 with the adaptive covers is not only more accurate but

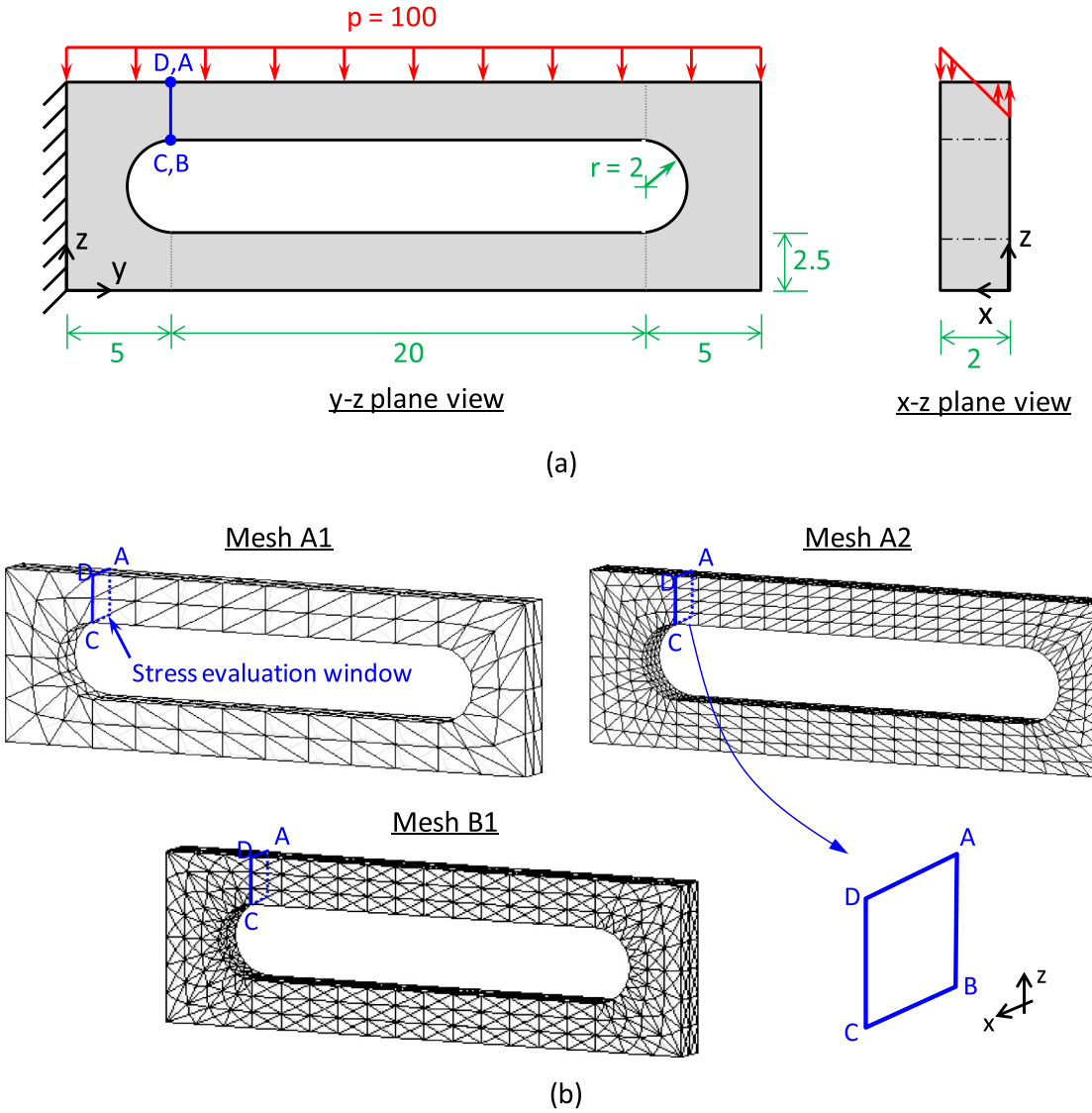

Fig. 17. Three-dimensional machine tool jig, (a) problem description, $E = 2e9$, $\nu = 0.3$, and (b) meshes used.

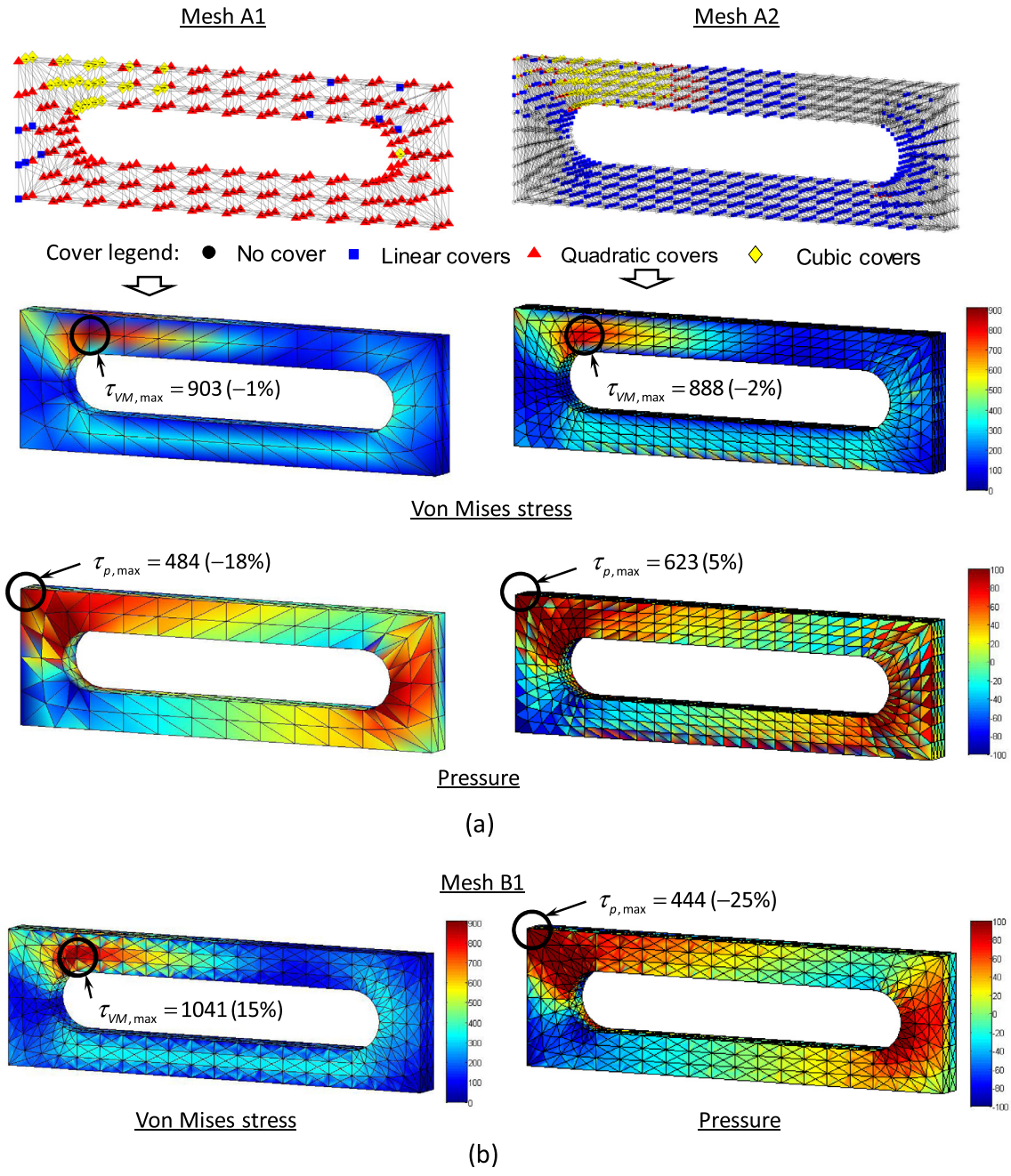

Fig. 18. Results of tool jig analyses, (a) adaptive scheme solutions using Meshes A1 and A2, and (b) quadratic element solution using Mesh B1.

also more efficient than the solution obtained using Mesh B1 with the quadratic element. In order to improve the stress results using the quadratic element, the mesh needs to be refined.

The von Mises stress result in Fig. 19 using the quadratic element looks better than when using covers with Meshes A1 and A2 because a symmetric mesh pattern has been used in Mesh B1, but for Mesh A2 the result is still reasonable.

5. Concluding remarks

The objective in this paper was to present a novel scheme to improve the finite element solutions when 3-node triangular elements and 4-node tetrahedral elements are used, respectively, in the two- and three-dimensional analyses of solids. Based on an error estimation technique, the scheme automatically selects the orders of the interpolation covers in the procedure presented in Ref. [1]. While the scheme actually improves the displacements and stresses, we focused in this paper on the results obtained for the stresses.

The procedure assumes that a reasonable traditional mesh has been used to obtain a first stress solution, and then applies enriched displacement interpolations using covers to improve the solution results. In the computations, the nodal point locations and mesh are not changed but simply the displacement interpolations are enriched over the cover regions pertaining to the nodes of the mesh. Different orders of enrichments can be applied over the nodal cover regions, and in this paper we presented a scheme to automatically select the order (ranging from 'no cover' to a 'cubic cover') depending on the approximate error, in a relative sense,

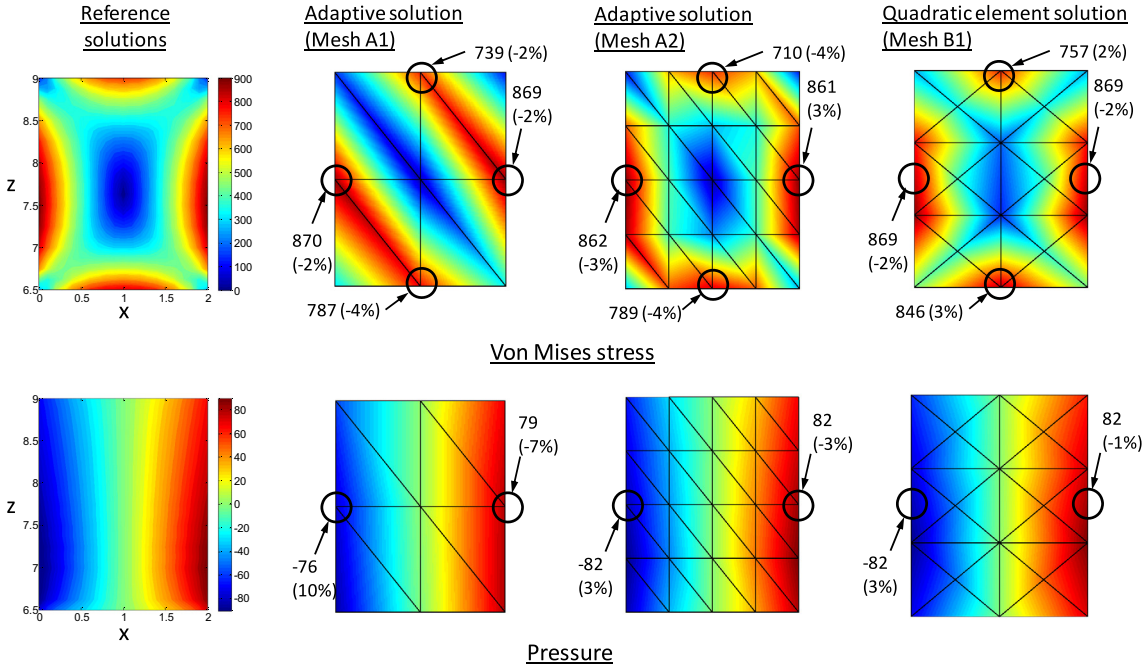

Fig. 19. Comparison of calculated von Mises stress and pressure on the stress evaluation window ABCD.

Table 5
Computational results for the two-dimensional tool jig problem.

	Adaptive scheme Mesh A1	Adaptive scheme Mesh A2	Quadratic element Mesh B1
DOFs (m_K)	8868 (888)	23,700 (1852)	35,085 (3333)
Computation time (s)	28	1288	1491
Cond($\underline{K}$)	2.2e8	1.7e8	3.2e8

measured at the node. The use of the procedure can decrease the computational effort but, in particular, can save human effort, since no new mesh is established. To illustrate the performance of the procedure we presented the results of various example solutions.

While there are these attractive attributes, we also pointed out that the initial (original) mesh must be reasonable; namely, the solution error can only be improved to some extent since the interpolation covers are only applied to improve the displacements (and hence stresses) and not the geometry. Throughout the analysis, the geometry is represented by the original mesh of triangular or tetrahedral elements. Also, some constants need to be chosen by the analyst for the scheme to automatically select the orders of interpolation covers. We proposed in the paper a rationale to select a set of reasonable constants.

Further developments of the scheme might focus on using also interpolation covers to improve the geometry interpolation, and to improve the method for the selection of the constants needed for the automatic solution, in particular for three-dimensional solutions. Of course, there are then many different areas where the scheme might be used and further developed, specifically for the analysis of plates and shells, see for example Ref. [10], fluid flows, and multi-physics problems.

References

[1] Kim J, Bathe KJ. The finite element method enriched by interpolation covers. Comput Struct 2013;116:35–49.
[2] Shi GH. Manifold method of material analysis. In: Transactions of the 9th army conference on applied mathematics and computing, Report No. 92–1, US Army Research, Office, 1991.
[3] Shi GH. Manifold method. In: Proceedings of the first international forum on discontinuous deformation analysis (DDA) and simulations of discontinuous media, New Mexico, USA; 1996. 52–204.
[4] Bathe KJ. Finite element procedures. Cambridge; 2006. [Revised 2014].
[5] Payen DJ, Bathe KJ. Improved stresses for the 4-node tetrahedral element. Comput Struct 2011;89:1265–73.
[6] Grätsch T, Bathe KJ. A posteriori error estimation techniques in practical finite element analysis. Comput Struct 2005;83:235–65.
[7] Bathe KJ, Zhang H. A mesh adaptivity procedure for CFD & fluid-structure interactions. Comput Struct 2009;87:604–17.
[8] Sussman T, Bathe KJ. Studies of finite element procedures—on mesh selection. Comput Struct 1985;21:257–64.
[9] Bucalem ML, Bathe KJ. The mechanics of solids and structures-hierarchical modeling and the finite element solution. Springer; 2011.
[10] Jeon HM, Lee PS, Bathe KJ. The MITC3 shell finite element enriched by interpolation covers. Comput Struct, submitted for publication.